

ORIGINAL ARTICLE

## Predictors of acute lymphopenia after radiotherapy for prostate cancer including pelvic node irradiation: results of a real-world prospective multi-centric study

V. Vavassori<sup>1†</sup>, M. Pavarini<sup>2†</sup>, L. Alborghetti<sup>2</sup>, S. Aimonetto<sup>3</sup>, A. Maggio<sup>4</sup>, V. Landoni<sup>5</sup>, P. Ferrari<sup>6</sup>, A. Bianculli<sup>7</sup>, E. Petrucci<sup>8</sup>, A. Cicchetti<sup>9</sup>, B. Farina<sup>10</sup>, M. G. Ubeira-Gabellini<sup>2</sup>, P. Salmoiraghi<sup>11</sup>, E. Moretti<sup>12</sup>, B. Avuzzi<sup>13</sup>, T. Giandini<sup>14</sup>, F. Munoz<sup>15</sup>, A. Magli<sup>16</sup>, B. Noris Chiorda<sup>13</sup>, G. Sanguineti<sup>17</sup>, J. M. Waskiewicz<sup>18</sup>, L. Rago<sup>19</sup>, D. Cante<sup>20</sup>, G. Girelli<sup>21</sup>, E. Villa<sup>1</sup>, N. G. Di Muzio<sup>22,23</sup>, T. Rancati<sup>9</sup>, C. Fiorino<sup>2\*</sup> & C. Cozzarini<sup>23</sup>

<sup>1</sup>Cliniche Gavazzeni-Humanitas, Radiotherapy Department, Bergamo; <sup>2</sup>IRCCS San Raffaele Scientific Institute, Medical Physics Department, Milano; <sup>3</sup>Ospedale Regionale Parini-AUSL Valle d'Aosta, Medical Physics Department, Aosta; <sup>4</sup>Istituto di Candiolo – Fondazione del Piemonte per l'Oncologia IRCCS, Medical Physics Department, Candiolo; <sup>5</sup>IRCCS Istituto Nazionale Tumori Regina Elena, UOSD Laboratorio di Fisica Medica e Sistemi Esperti, Roma; <sup>6</sup>Comprensorio Sanitario di Bolzano, Medical Physics Department, Bolzano; <sup>7</sup>IRCCS CROB, Medical Physics Department, Rionero in Vulture; <sup>8</sup>ASL TO4 Ospedale di Ivrea, Medical Physics Department, Ivrea; <sup>9</sup>Fondazione IRCCS Istituto Nazionale dei Tumori, Unit of Data Science, Milano; <sup>10</sup>Ospedale Degli Infermi, Medical Physics Department, Biella; <sup>11</sup>Cliniche Gavazzeni-Humanitas, Medical Physics Department, Bergamo; <sup>12</sup>Azienda Sanitaria Universitaria Friuli Centrale, Medical Physics Department, Udine; <sup>13</sup>Fondazione IRCCS Istituto Nazionale dei Tumori, Radiotherapy Department, Milano; <sup>14</sup>Fondazione IRCCS Istituto Nazionale dei Tumori, Medical Physics Department, Milano; <sup>15</sup>Ospedale Regionale Parini-AUSL Valle d'Aosta, Department of Radiation Oncology, Aosta; <sup>16</sup>Azienda Ospedaliero Universitaria S. Maria della Misericordia, Department of Radiotherapy, Udine; <sup>17</sup>IRCCS Regina Elena National Cancer Institute, Department of Radiation Oncology, Roma; <sup>18</sup>Comprensorio Sanitario di Bolzano, Radiotherapy, Bolzano; <sup>19</sup>IRCCS Crob, Radiotherapy, Rionero in Vulture; <sup>20</sup>ASL TO4 Ospedale di Ivrea, Radiotherapy, Ivrea; <sup>21</sup>Ospedale degli Infermi, Department of Radiotherapy, Biella; <sup>22</sup>Vita-Salute San Raffaele University, Milano; <sup>23</sup>IRCCS San Raffaele Scientific Institute, Department of Radiation Oncology, Milano, Italy

Available online 30 January 2026

**Background:** Acute lymphopenia (AL) is a clinically relevant concern in patients undergoing pelvic lymph-node irradiation (PNI) for prostate cancer (PCa) and reliable predictive models are not available. The purpose of the current analysis was to develop a predictive model of AL after PNI for PCa combining dosimetric and clinical information in a large, prospectively followed cohort.

**Materials and methods:** Clinical/dosimetry/blood test data from a multi-centric prospective study were available, including absolute lymphocyte count (ALC) at baseline, mid-point and radiotherapy (RT) end. Dose–volume histograms (DVHs) of the body and of pelvic bones were extracted, as well as the integral dose (ID) to the body. Lymph-nodal planning target volume (LN-PTV) and its cranial limit were also recovered. The current analysis focused on acute CTCAEv4.03 grade  $\geq 3$  (G3+) lymphopenia (ALC  $< 500/\mu\text{l}$ ), defined as the lowest count between baseline and mid-point or RT end. The patient population was split into training and validation cohorts, and a multivariable logistic regression model combining DVHs and clinical information was trained and validated.

**Results:** 700/887 patients with full 3D planning data and available baseline, mid-point and RT end counts were considered. 290 patients (41.4%) experienced acute G3+ lymphopenia. Both ID and pelvic bone DVH parameters were significantly associated with the endpoint. The two best resulting models included baseline ALC (OR = 0.999,  $P < 0.001$ ) and ID (Gy\*I) (OR = 1.003,  $P = 0.012$ ) or baseline ALC, cranial LN-PTV limit (OR = 1.019,  $P < 0.001$ ) and EQD2 to LN-PTV (OR = 1.095,  $P = 0.002$ ), when replacing ID with the cranial LN-PTV limit.

**Conclusions:** Severe AL after PNI for PCa is largely modulated by baseline ALC, with an independent role of the LN-PTV cranial limit or, alternatively, of ID, with the risk increasing by 5%-10% per  $10^2$  Gy\*I.

**Key words:** radiotherapy, hematological toxicity, lymphopenia, prostate cancer, integral dose, predictive models

\*Correspondence to: Dr Claudio Fiorino, Medical Physics, IRCCS San Raffaele Scientific Institute, Milano, Italy. Tel: +39-02-26432278  
E-mail: [fiorino.claudio@hsr.it](mailto:fiorino.claudio@hsr.it) (C. Fiorino).

<sup>†</sup>These authors share the first authorship.  
2949-8201/© 2026 The Authors. Published by Elsevier Ltd on behalf of European Society for Medical Oncology. This is an open access article under the CC BY-NC-ND license (<http://creativecommons.org/licenses/by-nc-nd/4.0/>).

### INTRODUCTION

The growing interest in radiation-induced immunosuppression derives from the increasing evidence of its importance as a side-effect and, above all, as a potentially negative factor in cancer treatment.<sup>1-8</sup> Acute lymphopenia is often experienced by patients undergoing radiotherapy, roughly proportional to the delivered dose and to the

extension of the treated volume.<sup>9</sup> The decrease of circulating lymphocytes due to their elimination in the blood, lymph nodes and other lymphoid organs may translate into a decrease in antitumor immune response.<sup>10</sup> After the post-irradiation acute phase, a recovery phase begins. This latter phase depends on dose, number of fractions and volume treated, and may result in absolute lymphocyte counts (ALC) remaining persistently lower than baseline for years after irradiation.<sup>9,11-14</sup> Modelling lymphopenia kinetics after radiotherapy is a complex task, owing to the interplay between blood circulation, exchange of lymphocytes between lymphoid organs and blood, and the delivered dose to different volumes at different times.<sup>9,15-17</sup> Simple models also exist, based on the measurement of ALC drop as a surrogate for the dose received in radiation accidents and adapted to the partial body irradiation case, typical of radiotherapy.<sup>18,19</sup>

It is also of note that, on one hand, the synergy between radiotherapy and immunotherapies could be significantly modulated by radiation-induced lymphopenia<sup>3,20-22</sup>; on the other hand, the combination of radiotherapy with chemotherapy may also enhance these effects, making it harder to distinguish the contribution of the different treating modalities to the potentially detrimental impact on cancer cure.<sup>23-26</sup> The case of adjuvant/neoadjuvant irradiation of large nodal areas is of high interest, as the benefit of radiotherapy could be counterbalanced by the detrimental effects of lymphopenia.

The balance between radiation-induced lymphopenia and treatment benefit is uncertain in the case of pelvic node irradiation (PNI) for prostate cancer (PCa). In fact, PNI has been found to have a positive impact in selected categories of patients, both in radical and post-prostatectomy settings.<sup>27,28</sup> The limited expected benefit for some categories of patients,<sup>29</sup> however, makes the potential long-term detrimental effects of radiation-induced lymphopenia on outcome/survival an issue. Moreover, as already reported by several studies,<sup>30-35</sup> the irradiation of pelvic bone marrow (BM) is also important. This helps in explaining, at least in part, the late persistence of lymphopenia due to the incomplete recovery of irradiated BM in producing blood components. Of note, PNI for PCa provides a valuable opportunity to study radiation-induced lymphopenia without any interaction with other immunotherapeutic/chemotherapeutic drugs.

A few studies have investigated predictors of acute lymphopenia after PNI for the treatment of PCa<sup>34</sup>; they reported that acute lymphopenia may be significant, with typically reported drops up to 20%-30% of the baseline values.<sup>11,36</sup> Findings from multi-centric prospective studies on sufficiently large cohorts, however, have never been reported.

A multi-centric study was started in 2012 (ClinicalTrials.gov#NCT02803086<sup>11,31,35-38</sup>) aiming to assess predictors of intestinal, hematological and urinary toxicity after PNI for PCa, delivered with intensity-modulated radiotherapy (IMRT) with both radical and post-prostatectomy

intent. This study represents, to our knowledge, the first multi-institute prospective trial explicitly aimed at thoroughly assessing and modeling lymphopenia after PNI for PCa. As data collection concerning acute lymphopenia was recently completed, the current study aimed to: (i) quantify dose-volume relationships between body/BM structures and acute severe lymphopenia; (ii) develop predictive models of acute lymphopenia combining dosimetry information with clinical predictors.

## MATERIALS AND METHODS

### *The multi-centric institutional trial*

After its activation at San Raffaele Institute, Milano, in September 2012, the Intestinal Hematologic Urinary Toxicity from Whole-Pelvis Radiotherapy (IHU-WPRT TOX) study aimed to develop predictive models of PNI-related toxicity across 14 Institutes treating PCa. Upon receiving the approval of the institutional review board of each of the participating institutes (ClinicalTrials.gov identifier NCT2803086), the multi-centric institutional trial enrolled 887 patients up to the end of 2021 and was planned to follow them for 5 years. Further details on the aims, patient characteristics, planning and volumes, dose/fractionation, delivery and methodology of the study have already been documented,<sup>36-38</sup> as well as the preliminary results regarding acute and late hematological toxicity (HT).<sup>31,35</sup> In short, all patients were treated with radical or post-prostatectomy IMRT including PNI. Conventional and moderate hypofractionation was permitted. The generation of PTVs from the corresponding clinical target volumes (CTVs) relative to prostate, seminal vesicles, prostatic and seminal vesicles bed was at the discretion of the treating radiation oncologist, provided that margins  $\leq 10$  mm were applied. Concerning the pelvic lymph nodes, the corresponding lymph-node planning treatment volume (PTVLN) was generated by isotropic expansion of 5-7 mm. With respect to the indication to PNI, it was at the discretion of the referring radiation oncologist of every participating institute. In general, it was usually recommended in the radical setting in the case of a probability of occult lymph-nodal metastases  $\geq 15\%$  according to the Roach nomogram.<sup>39</sup> In the post-prostatectomy PNI was chosen mostly in patients with seminal vesicle invasion, Gleason score  $\geq 7$ , pre-surgical prostate-specific antigen (PSA)  $> 10$  ng/ml and/or histologically positive lymph nodes at prostatectomy, or in the case of a PSA  $\geq 0.50$  ng/ml in the salvage setting.

### *Pelvic bone volume definition and DVH extraction*

Pelvic bone volumes were manually segmented, according to Mell et al.<sup>30</sup> The bone marrow of the ilium (BMILEUM) was defined from the superior border of the iliac crests to the top of the femoral heads; lumbosacral spine (BMLS) from the upper vertebral body where the PTVLN contours begin to the sacrum; lower pelvis (BMPELVIS) extending from the most superior border of the femoral heads to the

bottom of the ischial tuberosities; and whole pelvis (BMTOT), consisting of the union of the three sub-volumes.

To ensure comprehensive documentation of the PNI component of the treatment, relative planning data [planning computed tomography (CT), radiation therapy (RT) plan, RT dose and RT structure of Digital Imaging and Communications in Medicine (DICOM) files] were properly stored after generation.

The present study focused on the dose distribution associated with the first part of the treatment, due to the major impact of PNI, as previously reported.<sup>31,35</sup> This method disregards the minor contribution of small fields administered in the final phase of the treatment aimed at boosting the prostate or prostatic bed in the case of a sequential approach ( $n = 266$  patients out of 700), delivering boost doses in the range of 10–28 Gy at 1.8/2.0 Gy/fractions (fr).

In this context, dose–volume histograms (DVHs) of bones and body related to PNI were extracted in absolute values (cc) with a 1 Gy interval.

The daily dose prescribed to PTVLN was very similar across the institutions, with >95% of patients receiving a daily dose between 1.8 and 2 Gy and a maximum of 2.2 Gy/fr; thus, no correction for fractionation was applied.

The five lumbar (L5) vertebrae were delineated using TotalSegmentator, an open-source tool,<sup>40</sup> allowing the automatic computation of the cranial extent (mm) from the lower edge of the L5 vertebra (chosen arbitrarily as the reference plane) to the upper extremity of the PTVLN. This vertical distance, in millimeters, was determined by combining the baseline CT image with the contoured structures in Python, being positive if more cranial or negative if more caudal (arbitrary choice). This procedure eliminates any potential error and uncertainty in manually assessing the cranial PTVLN extent.

The integral dose (ID) to the body was calculated as the product between the mean dose (in Gy) and the volume (in l) of the body structure resulting from treatment planning.<sup>41–43</sup> The PTVLN volume (cc) was also retrieved and considered as a potential predictor.

### Endpoints and inclusion criteria definition

In accordance with the clinical trial protocol, blood tests were prospectively collected to monitor the absolute counts of white blood cells (WBC), lymphocytes (ALC), neutrophils (ANC), hemoglobin (Hb), platelets (PLT) and red blood cells (RBC) at baseline, RT mid-point and end, at 3 and 6 months after radiotherapy end, and thereafter every 6 months to 5 years after the conclusion of irradiation. Patients with complete baseline, radiotherapy mid-point and end blood tests, available planning and baseline clinical data were deemed eligible, resulting in a total of 700 patients available for the analysis.

According to the definition of CTCAE v4.03,<sup>44</sup> the primary endpoint of current analysis was acute grade  $\geq 3$  (G3+)

lymphopenia, defined as the lowest ALC count between radiotherapy mid-point and end  $< 500/\mu\text{l}$ .

### Identification of DVH predictors

In Figure 1, a diagram describes in detail the flow of the analyses.

First, all information available for the included patients was divided into training and validation sets, with an 80 : 20 split ratio, according to a 2a type TRIPOD validation.<sup>45</sup>

According to previously followed methods,<sup>31,35</sup> Mann–Whitney  $U$  tests were carried out on the training set to identify the regions of absolute DVHs of each BM and body structure that best discriminated patients with and without toxicity (i.e. corresponding to  $P$  values  $< 0.05$ ): only DVH values referring to these ‘significant’ regions were considered (with 1 Gy step) and named as VXGy. Finally, the number of the extracted DVH features was reduced by applying a correlation filter: when Spearman’s correlation coefficient was  $> 0.7$ , VXGy corresponding to the lowest  $P$  value with the Mann–Whitney  $U$  test was kept for further analyses. This procedure was necessary to limit redundancy, due to the large number of correlated features extracted from DVH.

### Analyses: model training and validation

The following prospectively collected clinical and dosimetric potential predictors were finally considered for model’s development: baseline WBC, ALC, ANC, age, body mass index (BMI), smoking, diabetes, hypertension, androgen deprivation therapy (ADT) (dichotomous, yes versus no and continuous, duration in months), the prescribed 2-Gy equivalent doses (EQD2, for  $\alpha/\beta = 3$  Gy) to PTVLN and to the prostatic bed/prostate PTVs, neoadjuvant ADT duration, prostatectomy (yes versus no), radiation technique (static versus arc/helical), hypofractionation (yes versus no), the pre-selected BM and body DVH parameters and ID. Due to their strong association with body DVH/ID (i.e. Spearman correlation  $\rho > 0.8$ ), PTVLN volume and its cranial limit were separately considered in a second analysis, excluding body DVH and ID: in this way, the possibility of using these geometric parameters as surrogates for body DVH/ID was explored. Of notice, the workflow described below was carried out twice, once for each covariate set of the twos just mentioned, resulting in two models: model 1, including ID and body DVH in the analysis; model 2: excluding them and including PTVLN volume and its cranial limit.

For the training set, univariate logistic regression was used to evaluate the impact of each covariate on the endpoint: variables with  $P$  value  $> 0.30$  were not considered for the next multivariable analysis. Then, a reduction of the candidate variables was further applied<sup>46</sup>: for variables with a significance level of  $P < 0.3$  in the univariate analysis, Spearman’s (or Pearson’s in the case of dichotomous variables) correlation coefficient was calculated. If two variables exhibited a high-level correlation ( $\rho > 0.8$ ), the variable with the largest  $P$  value was excluded.

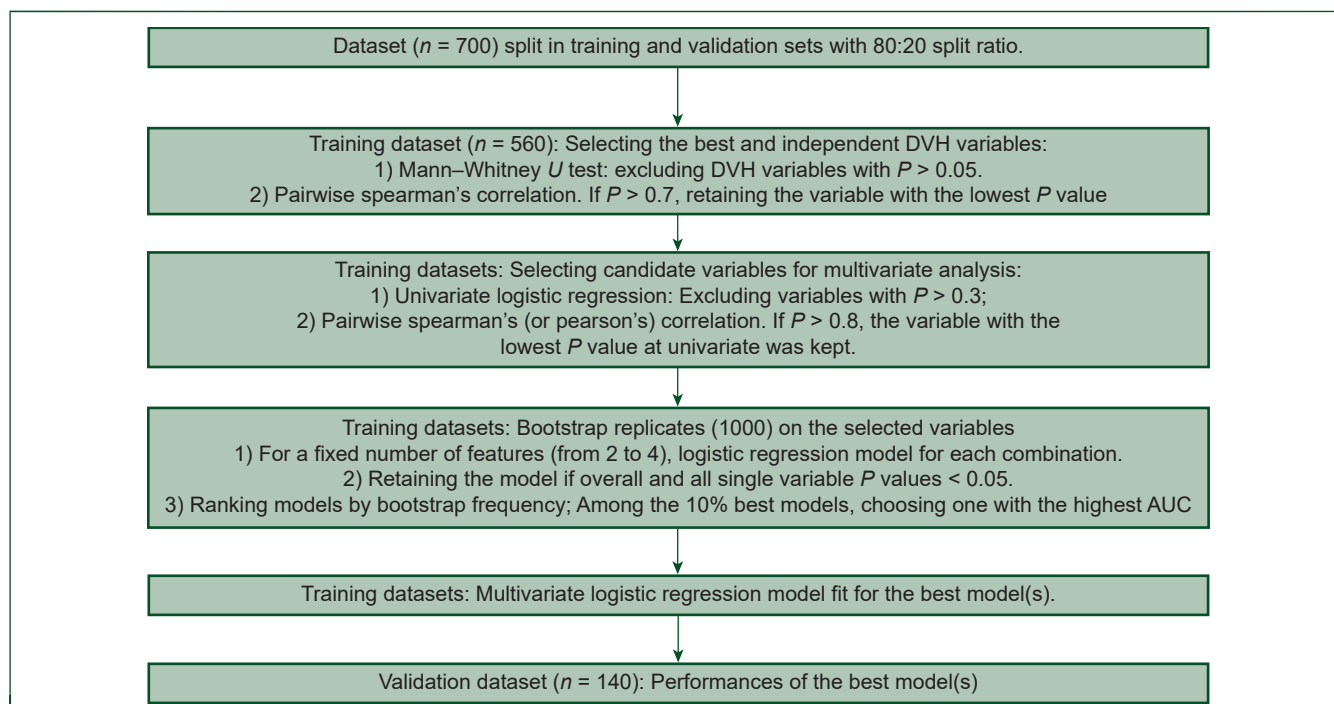


**Figure 1.** Flow diagram of the followed procedures for model's training and validation: the resulting number of patients and the number of variables were detailed at each step.

AUC, area under the curve; DVH, dose–volume histogram.

The feature selection in assessing the best multivariable models followed a bootstrap-based methodology. To emphasize the robustness of the resulting combination of variables, the maximum number of retained variables was constrained to a maximum of 4, corresponding to a number of variables per event of around 70, which was expected to be very robust.<sup>47</sup> One thousand bootstrap replicates were generated: for a fixed number of features progressively increased from 2 to 4, logistic regression models were fitted for each possible feature combination. For each bootstrap replicate, models were deemed to have good performance if the global  $P$  value and all single variable  $P$  values were  $<0.05$ . For each feature combination, the bootstrap frequency was calculated as the number of bootstrap replicates that met this criterion. Models were then ranked based on their bootstrap frequency and the top 10% feature combinations were considered: among them, the feature combination with the highest area under the ROC curve (ROC AUC) in the training cohort was chosen and the robustness of the model was later checked in the validation cohort.

The performances of the two resulting models were assessed based on the area under the precision-recall curve (PR AUC), ROC AUC, precision, sensitivity, specificity, F1class. For both models, the calibration plots were also calculated in the training and in the validation set, reporting slope, intercept and  $R^2$  values.

The preprocessing and modeling analysis were carried out with Python 3.7.9 (Python Software Foundation, <https://www.python.org/>) in-house code: medicalAI library in Medical Artificial Intelligence Toolkit for REsearch (mAIre).

In addition, a five-fold cross-validation approach was also followed to confirm the consistency of the models obtained following the above-described training/validation methodology.

## RESULTS

In the current analyses, 700 male patients met the selection criteria. **Table 1** provides a summary of the key clinical and dosimetry information. Two-hundred and ninety patients (41%) experienced acute G3+ lymphopenia.

According to Mann–Whitney  $U$  tests, significant differences between DVH with and without toxicity were found in the ranges V16–V57Gy for BODY, V52–V56Gy for BMTOT, V35–V68Gy for BMLS and V6–V39Gy for BMILEUM, as shown in **Supplementary Figure S1**, available at <https://doi.org/10.1016/j.esmorw.2025.100680>. After redundancy elimination, BMILEUM-V10Gy, BODY-V34Gy BMLS-V65Gy and BMLS-V56Gy were finally selected, together with the body ID.

**Supplementary Table S1**, available at <https://doi.org/10.1016/j.esmorw.2025.100680> shows the results of the univariate logistic regression analysis.

Sixteen and fourteen non-redundant and predictive features (for initial covariate sets with DVH/ID and lymph-nodal planning target volume (LN-PTV)/cranial extent, respectively) were identified in univariate analysis as eligible for entry into the subsequent training phase.

In **Table 2**, the resulting models are shown in detail; performance statistics for training and validation sets are presented in **Table 3**. When PTVLN volume and cranial L5

| Table 1. Summary of patient characteristics  |              |                           |                           |                         |
|--|--------------|---------------------------|---------------------------|-------------------------|
| Variable                                     | Class        | Postop (n = 454)          | Rad (n = 246)             | Total (n = 700)         |
| <b>Patient characteristics at baseline</b>   |              |                           |                           |                         |
| Age (years)                                  |              | 68 (62-72)                | 75 (70-78)                | 70 (65-75)              |
| BMI (kg/m <sup>2</sup> )                     |              | 26.1 (24.2-28.3)          | 26.7 (24.7-29.4)          | 26.2 (24.3-28.5)        |
| WBC (μl <sup>-1</sup> )                      |              | 6500 (5510-7710)          | 6900 (6100-7990)          | 6680 (5695-7805)        |
| ANC (μl <sup>-1</sup> )                      |              | 3788.8 (3020.7-4554.2)    | 3991.1 (3237.5-4882)      | 3875.3 (3088.3-4628)    |
| ALC (μl <sup>-1</sup> )                      |              | 1874.4 (1498-2337.8)      | 1959.6 (1644.6-2453.1)    | 1920.8 (1534.9-2399.9)  |
| <b>Comorbidities</b>                         |              |                           |                           |                         |
| Current or former smoker (cigarettes) (yes)  |              | 84/433 (19)               | 40/241 (17)               | 124/674 (18)            |
| Diabetes (yes)                               |              | 35/446 (8)                | 42/242 (17)               | 77/688 (11)             |
| Hypertension (yes)                           |              | 193/446 (43)              | 123/243 (51)              | 316/689 (46)            |
| <b>PCa characteristics</b>                   |              |                           |                           |                         |
| Initial PSA (ng/ml)                          |              | 9 (6-14)                  | 10.6 (6.4-18.9)           | 9.4 (6.2-15)            |
| Pre-RT PSA (ng/ml)                           |              | 0.25 (0.05-0.59)          | 6.5 (2.27-13)             | 0.59 (0.17-5.4)         |
| Gleason score                                | ISUP Group 1 | 23/444 (5)                | 8/243 (3)                 | 31/687 (5)              |
|  | ISUP Group 2 | 91/444 (20)               | 31/243 (13)               | 122/687 (18)            |
|  | ISUP Group 3 | 132/444 (30)              | 55/243 (23)               | 187/687 (27)            |
|  | ISUP Group 4 | 75/444 (17)               | 94/243 (39)               | 169/687 (25)            |
|  | ISUP Group 5 | 121/444 (27)              | 53/243 (22)               | 174/687 (25)            |
| T stage                                      | T1c          | 2/449 (0)                 | 30/245 (12)               | 32/694 (5)              |
|  | T2a          | 19/449 (4)                | 17/245 (7)                | 36/694 (5)              |
|  | T2b          | 13/449 (3)                | 33/245 (13)               | 46/694 (7)              |
|  | T2c          | 99/449 (22)               | 63/245 (26)               | 162/694 (23)            |
|  | T3a          | 148/449 (33)              | 72/245 (29)               | 220/694 (32)            |
|  | T3b          | 161/449 (36)              | 26/245 (11)               | 187/694 (27)            |
|  | T4           | 7/449 (2)                 | 4/245 (2)                 | 11/694 (2)              |
| N stage                                      | N0           | 223/450 (50)              | 145/226 (64)              | 368/676 (54)            |
|  | N1           | 160/450 (36)              | 34/226 (15)               | 194/676 (29)            |
|  | Nx           | 67/450 (15)               | 47/226 (21)               | 114/676 (17)            |
| <b>Radiotherapy data</b>                     |              |                           |                           |                         |
| Prescribed daily dose in Gy                  | @ PB/P-PTV   | 2.1 (2-2.4)               | 2.5 (2.4-2.7)             | 2.4 (2-2.5)             |
|  | @ LN-PTV     | 1.8 (1.8-1.9)             | 1.9 (1.8-2)               | 1.8 (1.8-1.9)           |
| Median EQD <sub>2</sub> <sub>3Gy</sub> in Gy | @ PB/P-PTV   | 72 (70-74)                | 80 (77-80)                | 74 (70.4-78)            |
|  | @ LN-PTV     | 50.2 (49.9-51.8)          | 52 (50.2-52.3)            | 51.1 (49.9-52)          |
| No. of fractions to PB/P-PTV                 |              | 33 (28-37)                | 28 (26-32)                | 30 (28-37)              |
| LN-PTV in cc                                 |              | 975.9 (781.5-1108.9)      | 781.8 (616.32-922.83)     | 889.1 (718.55-1070.45)  |
| Cranial L5-vertebrae-to-PTV-LN extent (mm)   |              | 40 (21.3-48)              | 27 (7.8-40)               | 36 (15-45)              |
| RT technique                                 | SS-IMRT      | 28/452 (6)                | 6/245 (2)                 | 34/697 (5)              |
|  | TOMO         | 169/452 (37)              | 94/245 (38)               | 263/697 (38)            |
|  | VMAT         | 255/452 (56)              | 145/245 (59)              | 400/697 (57)            |
| Dose to 1% of volume BMILEUM (Gy)            |              | 54 (52-56)                | 54 (51-56)                | 54 (52-56)              |
| Dose to 1% of volume BMLS (Gy)               |              | 54 (53-56)                | 55 (52-57)                | 55 (52.8-56)            |
| Dose to 1% of volume BMPELVIS (Gy)           |              | 62 (60-68)                | 68 (60-70)                | 65 (60-69)              |
| Dose to 1% of volume BMTOT (Gy)              |              | 62 (60-68)                | 68 (61-70)                | 65 (60-69)              |
| Dose to 1% of volume BODY (Gy)               |              | 64 (61-70)                | 72 (69-73)                | 68 (61-72)              |
| Mean dose to BMILEUM (Gy)                    |              | 28.3 (26.3-30.5)          | 26.8 (24.5-29.5)          | 27.9 (25.5-30.1)        |
| Mean dose to BMLS (Gy)                       |              | 36 (31.6-39.5)            | 33.4 (29.1-38.8)          | 35.1 (30.7-39.4)        |
| Mean dose to BMPELVIS (Gy)                   |              | 28.9 (25.5-31.9)          | 26.4 (23.9-29.4)          | 27.9 (25-31.2)          |
| Mean dose to BMTOT (Gy)                      |              | 31 (27.5-33.1)            | 28.4 (26.4-30.9)          | 30.1 (27-32.5)          |
| Mean dose to BODY (Gy)                       |              | 14.1 (12.3-15.9)          | 13.4 (11.4-15.4)          | 13.8 (12-15.7)          |
| Volume BMILEUM (cc)                          |              | 493.3 (447.9-546.6)       | 503.2 (452.5-565.4)       | 496 (449.4-549.8)       |
| Volume BMLS (cc)                             |              | 453.1 (394.6-517.3)       | 416.6 (374.3-480.8)       | 436.9 (383.6-506.6)     |
| Volume BMPELVIS (cc)                         |              | 715 (650.7-777.9)         | 709.4 (642.5-765.5)       | 712.6 (648.3-776.4)     |
| Volume BMTOT (cc)                            |              | 1659.3 (1502.1-1820.9)    | 1621.8 (1481.4-1781.9)    | 1646.2 (1493.8-1808.1)  |
| Volume BODY (cc)                             |              | 26764.6 (22760.2-31884.1) | 27572.5 (23332.5-32147.8) | 27060.6 (22834-32016.7) |
| <b>Hormonal therapy</b>                      |              |                           |                           |                         |
| ADT  | AA only      | 31/224 (14)               | 28/218 (13)               | 59/442 (13)             |
|  | CAB          | 33/224 (15)               | 24/218 (11)               | 57/442 (13)             |
|  | LH-RH        | 160/224 (71)              | 166/218 (76)              | 326/442 (74)            |
| ADT duration in months                       |              | 24 (23-24)                | 24 (24-25)                | 24 (24-24)              |
| Neoadjuvant ADT                              |              | 2 (1-3)                   | 2 (1-4)                   | 2 (1-3)                 |

Continued

| Table 1. Continued         |              |                  |               |                 |
|----------------------------|--------------|------------------|---------------|-----------------|
| Variable                   | Class        | Postop (n = 454) | Rad (n = 246) | Total (n = 700) |
| <b>Surgery</b>             |              |                  |               |                 |
| Type                       | Laparoscopic | 50/441 (11)      |               | 50/441 (11)     |
|                            | Open         | 238/441 (54)     |               | 238/441 (54)    |
|                            | Robotic      | 153/441 (35)     |               | 153/441 (35)    |
| Surgical margins           | Negative     | 188/431 (44)     |               | 188/564 (33)    |
|                            | Positive     | 235/431 (55)     |               | 235/564 (42)    |
|                            | n.a.         | 8/431 (2)        |               | 141/564 (25)    |
| No. of lymph nodes removed |              | 13 (7-21)        |               | 12 (4-20)       |

Data for categorical variables are presented as counts (%), and for continuous variables as median values (inter-quartile range).

ADT, androgen deprivation therapy; ALC, absolute lymphocyte count; ANC, absolute neutrophil count; BMI, body mass index; BMILEUM, bone marrow of the ilium; BMLS, bone marrow of the lumbosacral spine; BMPELVIS, bone marrow of the lower pelvis; BMTOT, bone marrow of the whole pelvis; Gy, Gray; IQR, interquartile range; LN-PTV, lymph-nodal planning target volume; N, node; n.a., not available; PB/P-PTV, prostatic bed/prostate planning target volume; PCa, prostate cancer; Postop, post-prostatectomy; PSA, prostate-specific antigen; Rad, radical radiotherapy; RT, radiotherapy; T, tumor; WBC, absolute white blood cell count.

vertebra to PTVLN extent were considered (in place of body DVH/ID), ALC at baseline, EQD2<sub>3Gy</sub> at LN-PTV (Gy) and cranial limit led to the best performing model (model 1). When considering body DVH/ID, the resulting model (model 2) retained ALC at baseline and ID. Bootstrap frequencies were 903/1000 and 729/1000 for the first and second model, respectively. ROC AUC scored 0.757/0.752 and 0.738/0.712, for the training/validation cohorts of model 1/model 2, respectively.

The resulting calibration plots on the validation set were shown in Figure 2. The calibration showed high R<sup>2</sup> values, slightly better for model 1 (0.94 and 0.84 for model 1 and 2, respectively). Of note, the resulting calibration plots in the training set showed similar performances (i.e. R<sup>2</sup> values equal to 0.95 and 0.77, Supplementary Material, available at <https://doi.org/10.1016/j.esmorw.2025.100680>).

In Figure 3, aiming to better represent the combined impact of baseline ALC and ID, the risk for increasing values of ID was shown, stratified by values of ALC at baseline, chosen as the quartiles of its distribution. The values of ID corresponding to 25% risk were <10<sup>2</sup>, 1.6 × 10<sup>2</sup>, 3 × 10<sup>2</sup> and 4.8 × 10<sup>2</sup> GyL for ALC baseline ≤1536 μl<sup>-1</sup>, between 1536 and 1920 μl<sup>-1</sup>, between 1920 and 2400 μl<sup>-1</sup> and

>2400 μl<sup>-1</sup>, respectively; the corresponding ID values for 50% risk were 1.2 × 10<sup>2</sup>, 4.7 × 10<sup>2</sup>, 6.0 × 10<sup>2</sup> and 7.8 × 10<sup>2</sup> GyL.

The results of the five-fold cross-validation are reported in the Supplementary Material, available at <https://doi.org/10.1016/j.esmorw.2025.100680>: the selected variables of the two models as well as their relative importance were substantially confirmed. The only (minor) difference concerns model 2, where the procedure retained EQD2<sub>3Gy</sub> @ LN-PTV (Gy), in addition to baseline ALC and ID, as happened for model 1. The average performances of the models were in line with the ones reported in Table 1 (see Supplementary Table S3, available at <https://doi.org/10.1016/j.esmorw.2025.100680>).

## DISCUSSION

The growing interest in lymphopenia as a potentially detrimental factor in cancer cure has only partially involved the case of PNI for PCa. While the association between lymphopenia and poorer outcome has been reported for several tumors, such as glioblastoma, head-neck, pancreatic, esophageal, lung and stomach cancers,<sup>2-8</sup> this is not

| Table 2. Results of the multivariable logistic regression analysis fit for acute G3+ lymphopenia |                                       |                |       |                 |
|--|---------------------------------------|----------------|-------|-----------------|
| <b>Model 1</b>   |                                       |                |       |                 |
| Predictors   | Coeff ± standard error                | P value        | OR    | 95% CI          |
| Baseline ALC (μl <sup>-1</sup> )   | -0.0013 ± 0.0002                      | <0.001         | 0.999 | (0.998-0.999)   |
| Cranial extent (mm)  | 0.019 ± 0.005                         | <0.001         | 1.019 | (1.010-1.028)   |
| EQD2 <sub>3Gy</sub> @ LN-PTV (Gy)  | 0.091 ± 0.029                         | 0.002          | 1.095 | (1.035-1.159)   |
| Intercept  | -3.159 ± 1.577                        | 0.045          |       |                 |
| LLR P < 0.001  | R <sup>2</sup> <sub>NAG</sub> = 0.218 | PR AUC = 0.674 |       | ROC AUC = 0.757 |
| <b>Model 2</b>   |                                       |                |       |                 |
| Predictors   | Coeff ± standard error                | P value        | OR    | 95% CI          |
| Baseline ALC (μl <sup>-1</sup> )   | -0.0012 ± 0.0002                      | <0.001         | 0.999 | (0.998-0.999)   |
| Integral dose BODY (GyL)   | 0.0031 ± 0.0013                       | 0.012          | 1.003 | (1.001-1.006)   |
| Intercept  | 0.938 ± 0.571                         | 0.101          |       |                 |
| LLR P value <0.001   | R <sup>2</sup> <sub>NAG</sub> = 0.181 | PR AUC = 0.632 |       | ROC AUC = 0.738 |

ALC, absolute lymphocyte count; cranial extent, cranial extent from the L5 vertebrae lower edge to the PTVLN upper extremity (mm); EQD2<sub>3Gy</sub> @ LN-PTV, prescribed 2-Gy equivalent dose (EQD2, for α/β = 3Gy) to the pelvic lymph nodes/lymph-nodal area (Gy); integral dose BODY, the product of the mean dose to the structure and the irradiated volume (GyL); LN-PTV, lymph-nodal planning target volume; LLR P value, log-likelihood ratio P value; PR AUC, area under the precision-recall curve; R<sup>2</sup><sub>NAG</sub>, Nagelkerke's pseudo-R-squared; ROC AUC, area under the receiving operating characteristic curve.

| Table 3. Performance statistics for training and validation sets of the multivariable logistic regression analysis for acute G3+ lymphopenia |   |             |             |            |            |         |        |
|--|---|-------------|-------------|------------|------------|---------|--------|
|  | Precision   | Specificity | Sensitivity | F1 class 0 | F1 class 1 | ROC AUC | PR AUC |
| Model 1  | Baseline ALC ( $\mu\text{l}^{-1}$ ) and cranial extent (mm) and EQD23Gy @ LN-PTV (Gy) |             |             |            |            |         |        |
| Training   | 0.631   | 0.716       | 0.704       | 0.746      | 0.665      | 0.757   | 0.674  |
| Validation   | 0.557   | 0.592       | 0.736       | 0.667      | 0.634      | 0.752   | 0.656  |
| Model 2  | Baseline ALC ( $\mu\text{l}^{-1}$ ) and integral dose BODY (GyL)                      |             |             |            |            |         |        |
| Train  | 0.658   | 0.782       | 0.605       | 0.762      | 0.631      | 0.738   | 0.631  |
| Validation   | 0.593   | 0.688       | 0.648       | 0.711      | 0.619      | 0.712   | 0.629  |

ALC, absolute lymphocyte count; LN-PTV, lymph-nodal planning target volume; PR AUC, area under the precision-recall curve; ROC AUC, area under the receiving operating characteristic curve.

yet the case for PCa patients. The main reason for this lack likely depends on the excellent survival that makes it necessary to follow large cohorts of patients for many years to clearly detect any potential detrimental effect of radiation-induced lymphopenia. By contrast, growing evidence shows that PNI has a positive impact on selected patient categories in terms of biochemical relapse-free survival.<sup>28,29</sup> This highlights the issue of balancing the long-term effects: while PNI can sterilize micro-metastases in pelvic nodes, it can also cause radiation-induced immunosuppression, leading to persistent lymphopenia that may hinder further therapies for patients experiencing relapse.

Lymphopenia was recently found to be still significant 2 years after PNI,<sup>35</sup> and preliminary (unpublished) findings of our IHU study confirm that complete recovery is far from being reached even 5 years after radiotherapy. While persistent lymphopenia is likely the most substantial effect, acute lymphopenia is the first sign of the severity of radiation-induced immunosuppression, often leading to an incomplete restoration of baseline ALC values. It is therefore unsurprising that

severe acute lymphopenia was found to be associated with 1- and 2-year lymphopenia.<sup>31,35</sup> A careful assessment of the predictors of acute lymphopenia, as carried out in the current study, is therefore of paramount importance.

Additionally, potential harm in terms of increased risk and/or severity of side-effects due to lymphopenia should not be underestimated. This includes the potential impact on fatigue and quality of life (QoL).<sup>6,43</sup>

The present study represents the first large multi-centric prospective study on the topic, involving 887 patients enrolled in 14 institutions over several years and treated with PNI using IMRT. While the follow-up is not yet sufficiently mature to carry out the final analyses dealing with persistent lymphopenia at 5 years, the current findings on acute lymphopenia should be considered definitive, reporting the findings relative to 700 patients with full dosimetry and clinical information (i.e. baseline, mid- and end-RT ALC counts) available.

The rate of acute G3+ lymphopenia (41.4%) was in line with other investigations<sup>36,48,49</sup> and with our previous

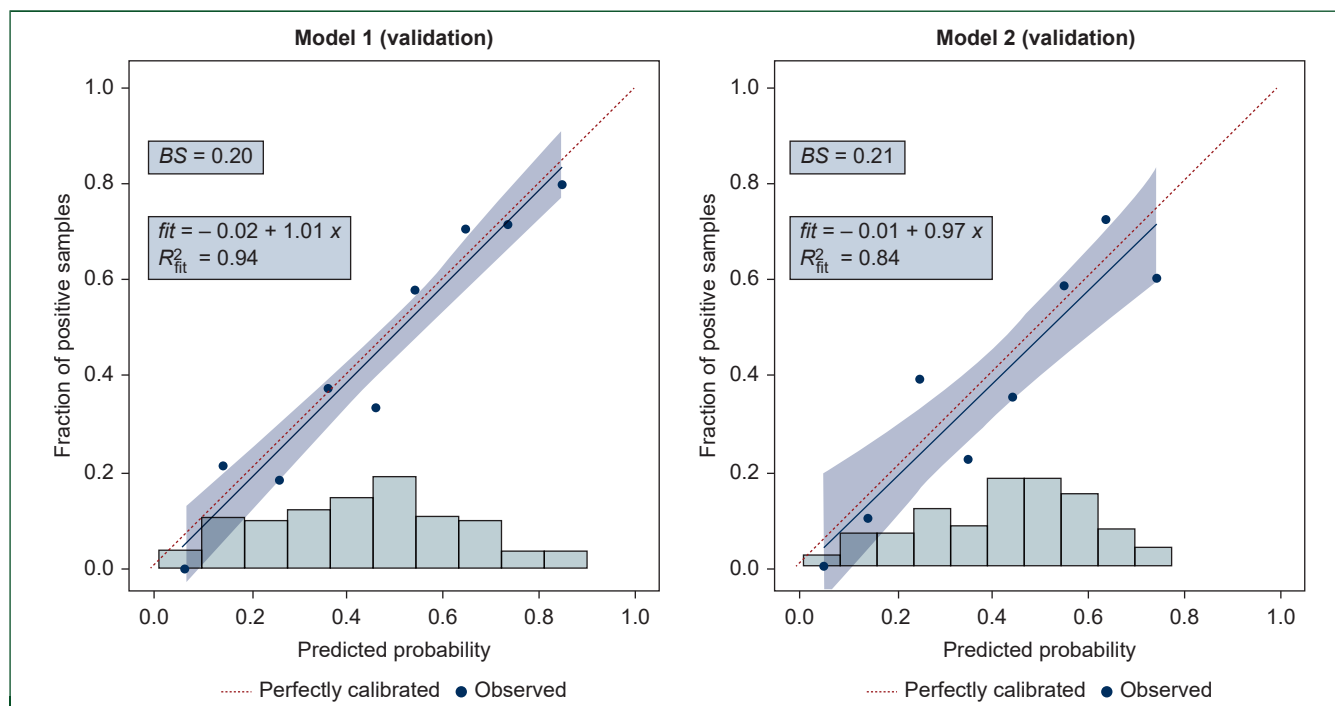
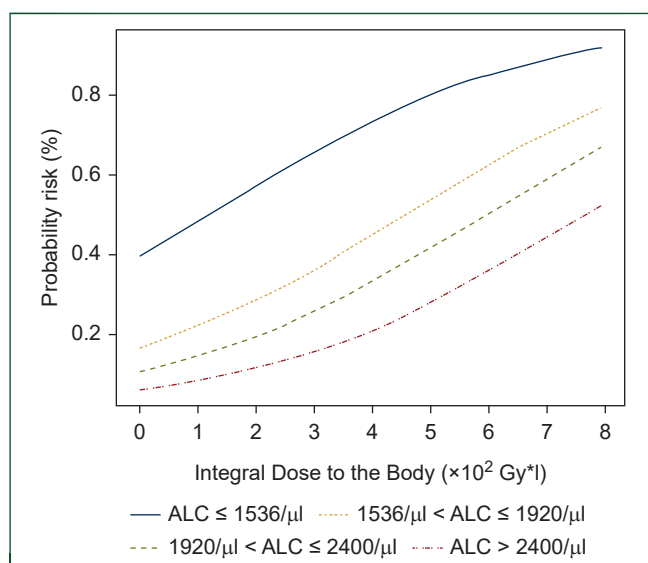


Figure 2. Calibration plots of model 1 (top) and model 2 (down), as reported in Table 2, on the validation cohort. According to the cohort's quartiles, the rate of predicted patient's rate against the true rates were compared: slope, intercept and  $R^2$  are reported.



**Figure 3. Probability risk (%) for acute G3+ lymphopenia at increasing levels of integral dose to the body ( $\times 10^2$  Gy\*), stratified by the quartiles of ALC at baseline distribution.** Logistic curves with variables ID and categorized ALC at baseline were fitted, according to model 2. The risk for each of the quartiles (i.e. the probability of having a positive outcome) was calculated as  $1/(1+\exp[-\text{logit}(p)])$  with  $\text{logit}(p) = b_0 + b_1 X_1$ , where  $b_0$  is the coefficient of the intercept,  $b_1$  the coefficient relating to the quartile and  $X_1$  its dichotomous variable. ALC, absolute lymphocyte count; ID, integral dose.

single institution reports.<sup>11,31</sup> The large numbers guaranteed a high robustness of the resulting prediction models both in the training and in the validation cohorts with high performances in terms of calibration, well captured by the  $R^2$  values of the reported calibration plots.

As previously reported in our first mono-centric pilot study,<sup>31</sup> the baseline ALC value is the major predictor of G3+ acute lymphopenia. A similar result was found for 2-year lymphopenia in a subgroup of the patients considered here.<sup>35</sup> This result was not unexpected, as the drop of ALC from baseline values is expected to follow a (roughly) exponential pattern.<sup>18,19</sup> Consequently, the probability that the nadir will fall below the G3+ threshold ( $<500 \mu\text{l}^{-1}$ ) critically depends on the baseline count.

While no other clinical factors showed association with lymphopenia, the analysis regarding dosimetry predictors showed that both body and BM DVHs are associated with an increased risk of G3+ lymphopenia; when applying rigorous selection of the most robust and predictive parameters, however, body dosimetry seems to outperform BM dosimetry, with ID appearing as the best predictor. This result is not unexpected: body and BM dose–volume parameters are cross-correlated, which explains the reported associations between BM DVHs and acute lymphopenia in few other studies.<sup>31,34</sup> Given a fixed number of fractions and delivered dose, body DVHs/ID are expected to be highly associated with ALC drop, representing a surrogate for the dose directly received by lymphocytes.<sup>16–19,48</sup> The lower predictive role of BM DVH is expected, as acute lymphopenia is more susceptible to the dose received by the circulating lymphocytes.<sup>9</sup> Interestingly, when focusing on 2-year late G2+ lymphopenia, BM DVHs were found to outperform predictions against body ID/DVH, as recently

reported by Pavarini et al.<sup>35</sup> on the same population of the current study; in the same paper, an independent role of baseline ALC and of acute G3+ lymphopenia was clearly found. This is in line with the consolidated assumption that long-term lymphopenia is primarily due to the lack of active BM due to radiation-induced depletion. Moreover, acute G3+ lymphopenia is relevant in predicting an increased risk of late lymphopenia, suggesting that any attempt to reduce acute lymphopenia translates into a reduced risk of persistent lymphopenia.

It is also important to underline that, when replacing body dosimetry with geometrical surrogates (i.e. cranial limit of PTVLN, PTVLN volume), the best performing parameters, apart from baseline ALC, are the cranial PTV limit and EQD2. Of these, the cranial limit performed best. The performance of the corresponding model is slightly better than that of the model combining baseline ALC and ID. This latter result is likely due to the intrinsic limitations of using ID as a surrogate for the radiation dose to the lymphocytes. This should also explain the better performance of the cranial limit of PTV, which makes this metric less sensitive to the individual variability of the meaning of ID. Although more investigation is warranted to better model ALC drop by taking individual weight into account, the finding regarding the impact of cranial limit may have immediate application. It suggests that reducing the risk of G3+ acute lymphopenia can be achieved by simply limiting the cranial PTV limit in patients with low baseline ALC values. Moreover, the explicit inclusion of ID and BM sparing into plan optimization could have potential in reducing acute and persistent lymphopenia.<sup>50,51</sup> Even the use of protons has been shown to largely reduce ID compared with advanced photon modalities.<sup>52,53</sup> By contrast, our findings suggest that the potential of reducing acute lymphopenia during plan optimization is limited as it mostly depends on the baseline value. As lymphopenia may counterbalance the positive effects of cell killing in micro-metastases in terms of a potential hampering of further therapies and impaired QoL, care should be taken before prescribing PNI, especially for categories of patients in whom the benefit of PNI may be limited or has not yet been fully established.<sup>29</sup>

Our study has several limitations: the variable selection procedure has some limits as it cannot completely guarantee to miss potential predictors. By contrast, the substantial confirmation of our findings when applying five-fold cross-validation as well as our pre-selection procedure of the variables suggest high robustness of the results. As a matter of fact, the whole methodology gave more emphasis to model's robustness than model's performances, restricting the choice to models combining a small number of variables (i.e.  $\leq 4$ ).

Other limitations concern the lack of potentially relevant predictors (such as genetic information) and the lack of more detailed spatial description of the dose distribution, possibly captured by more advanced 'voxel-wise' methodologies.<sup>54</sup> Another major issue remains the lack of evidence, as previously mentioned, of any clinically relevant impact of acute lymphopenia after PNI for PCa. The

availability of patient-reported urinary and bowel toxicity information for all patients should, however, permit exploration of their potential interplay with lymphopenia. Moreover, the current cohort is also precious to investigate the above-mentioned potential detriment of radiation-induced lymphopenia in terms of biochemical relapse-free and overall survival. These analyses are planned and promise to enlighten the topic with potentially relevant impact of PNI practice in PCa radiotherapy.

### Conclusions

The current study reported the results of the largest prospective trial dedicated to lymphopenia after PNI for PCa in a modern, multi-institute cohort of patients treated with IMRT. In addition, an assessment of a predictive model of acute lymphopenia, including dose–volume relationships, was carried out. Acute severe lymphopenia after PNI for PCa was found to affect about 40% of patients. While the baseline ALC value emerged as the major predictor, the risk is independently modulated by ID as well: the risk was quantified to increase on the order of 5%-10% per  $10^2$  Gy $\cdot$ l. Replacing ID with the cranial limit of PTV and EQD2 resulted in an alternative predictive model with similar, if not slightly better, performances.

Moderate, although significant, mitigation of severe acute lymphopenia could be obtained by limiting the cranial extension of PTV, especially for patients with low baseline ALC value. Further research in quantifying the association between acute and persistent lymphopenia against outcome and QoL after PNI is warranted.

### ACKNOWLEDGEMENTS

Frank Begg is gratefully acknowledged.

### FUNDING

This work was supported by grants from Associazione Italiana Ricerca Cancro (AIRC) Investigational Grant [grant number 14603].

### DISCLOSURE

The authors have declared no conflicts of interest.

### REFERENCES

- Raben M, Walach N, Galili U, Schlesinger M. The effect of radiation therapy on lymphocyte subpopulations in cancer patients. *Cancer*. 1976;37:1417-1421.
- Damen PJJ, Kroese TE, van Hillegersberg R, et al. The influence of severe radiation-induced lymphopenia on overall survival in solid tumors: a systematic review and meta-analysis. *Int J Radiat Oncol Biol Phys*. 2021;15:936-948.
- Venkatesulu BP, Mallick S, Lin SH, Krishnan S. A systematic review of the influence of radiation-induced lymphopenia on survival outcomes in solid tumors. *Crit Rev Oncol. Hematol*. 2018;123:42-51.
- Terrones-Campos C, Ledergerber B, Vogelius IR, et al. Lymphocyte count kinetics, factors associated with the end-of-radiation-therapy lymphocyte count, and risk of infection in patients with solid malignant tumors treated with curative-intent radiation therapy. *Int J Radiat Oncol Biol Phys*. 2019;105:812-823.

- Upadhyay R, Venkatesulu BP, Giridhar P, et al. Risk and impact of radiation related lymphopenia in lung cancer: a systematic review and meta-analysis. *Radiother Oncol*. 2021;157:225-233.
- Venkatesulu BP, Chan DP, Giridhar P, et al. A systematic review and meta-analysis of the impact of radiation-related lymphopenia on outcomes in pancreatic cancer. *Future Oncol*. 2022;18:1885-1895.
- Tang C, Liao Z, Gomez D, et al. Lymphopenia association with gross tumor volume and lung V5 and its effects on non-small cell lung cancer patient outcomes. *Int J Radiat Oncol Biol Phys*. 2014;89:1084-1091.
- Wild AT, Ye X, Ellsworth SG, et al. The association between chemoradiation-related lymphopenia and clinical outcomes in patients with locally advanced pancreatic adenocarcinoma. *Am J Clin Oncol*. 2015;38:259-265.
- Paganetti H. A review on lymphocyte radiosensitivity and its impact on Radiotherapy. *Front Oncol*. 2023;13:1201500.
- Grassberger C, Ellsworth SG, Wilks MQ, Keane FK, Loeffler JS. Assessing the interactions between radiotherapy and antitumour immunity. *Nat Rev Clin Oncol*. 2019;16:729-745.
- Cozzarini C, Noris Chiorda B, Sini C, et al. Hematologic toxicity in patients treated with postprostatectomy whole-pelvis irradiation with different intensity modulated radiation therapy techniques is not negligible and is prolonged: preliminary results of a longitudinal, observational study. *Int J Radiat Oncol Biol Phys*. 2016;95:690-695.
- Velardi E, Tsai JJ, van den Brink MRM. T cell regeneration after immunological injury. *Nat Rev Immunol*. 2021;21:277-291.
- Terrones-Campos C, Ledergerber B, Vogelius IR, Helleberg M, Specht L, Lundgren J. Hematological toxicity in patients with solid malignant tumors treated with radiation – temporal analysis, dose response and impact on survival. *Radiother Oncol*. 2021;158:175-183.
- O'Toole C, Unsgaard B. Clinical status and rate of recovery of blood lymphocyte levels after radiotherapy for bladder cancer. *Cancer Res*. 1979;39:840-843.
- Ebrahimi S, Lim G, Hobbs BP, Lin SH, Mohan R, Cao W. A hybrid deep learning model for forecasting lymphocyte depletion during radiation therapy. *Med Phys*. 2022;49:3507-3522.
- Shin J, Xing S, McCullum L, et al. HEDOS-a computational tool to assess radiation dose to circulating blood cells during external beam radiotherapy based on whole-body blood flow simulations. *Phys Med Biol*. 2021;66. <https://doi.org/10.1088/1361-6560/ac16ea>.
- McCullum L, Shin J, Xing S, et al. Predicting severity of radiation induced lymphopenia in individual proton therapy patients for varying dose rate and fractionation using dynamic 4-dimensional blood flow simulations. *Int J Radiat Oncol Biol Phys*. 2023;116:1226-1233.
- Goans RE, Holloway EC, Berger ME, Ricks RC. Early dose assessment following severe radiation accidents. *Health Phys*. 1997;72:513-518.
- Ellsworth SG, Yalamanchali A, Lautenschlaeger T, et al. Lymphocyte depletion rate as a biomarker of radiation dose to circulating lymphocytes during fractionated partial-body radiation therapy. *Adv Radiat Oncol*. 2022;7:100959.
- Eckert F, Schaedle P, Zips D, et al. Impact of curative radiotherapy on the immune status of patients with localized prostate cancer. *Oncoimmunology*. 2018;7(11):e1496881.
- Ménétrier-Caux C, Ray-Coquard I, Blay JY, Caux C. Lymphopenia in cancer patients and its effects on response to immunotherapy: an opportunity for combination with cytokines? *J Immunother Cancer*. 2019;7(1):85.
- Lambin P, Lieveise RIV, Eckert F, et al. Lymphocyte-sparing radiotherapy: the rationale for protecting lymphocyte-rich organs when combining radiotherapy with immunotherapy. *Semin Radiat Oncol*. 2020;30:187-193.
- Mauch P, Constine L, Greenberger J, et al. Hematopoietic stem cell compartment: acute and late effects of radiation therapy and chemotherapy. *Int J Radiat Oncol Biol Phys*. 1995;31:1319-1339.
- Wu ES, Oduyabo T, Cobb LP, et al. Lymphopenia and its association with survival in patients with locally advanced cervical cancer. *Gynecol Oncol*. 2016;140:76-82.
- Mell LK, Kochanski JD, Roeske JC, et al. Dosimetric predictors of acute hematologic toxicity in cervical cancer patients treated with

- concurrent cisplatin and intensity-modulated pelvic radiotherapy. *Int J Radiat Oncol Biol Phys.* 2006;66:1356-1365.
26. Klopp AH, Moughan J, Portelance L, et al. Hematologic toxicity in RTOG 0418: a phase 2 study of postoperative IMRT for gynecologic cancer. *Int J Radiat Oncol Biol Phys.* 2013;86:83-90.
  27. Murthy V, Maitre P, Kannan S, et al. Prostate-only versus whole-pelvic radiation therapy in high-risk and very high-risk prostate cancer (POP-RT): outcomes from phase III randomized controlled trial. *J Clin Oncol.* 2021;39:1234-1242.
  28. Pollack A, Karrison TG, Balogh AG, et al. The addition of androgen deprivation therapy and pelvic lymph node treatment to prostate bed salvage radiotherapy (NRG Oncology/RTOG 0534 SSPORT): an international multicentre, randomized phase 3 trial. *Lancet.* 2022;399:1886-1901.
  29. Cozzarini C, Olivieri M, Magli A, et al. Accurate prediction of long-term risk of biochemical failure after salvage radiotherapy including the impact of pelvic node irradiation. *Radiother Oncol.* 2022;175:26-32.
  30. Mell LK, Schomas DA, Salama JK, et al. Association between bone marrow dosimetric parameters and acute hematologic toxicity in anal cancer patients treated with concurrent chemotherapy and intensity-modulated radiotherapy. *Int J Radiat Oncol Biol Phys.* 2008;70:1431-1437.
  31. Sini C, Fiorino C, Perna L, et al. Dose—volume effects for pelvic bone marrow in predicting hematological toxicity in prostate cancer radiotherapy with pelvic node irradiation. *Radiother Oncol.* 2016;118:79-84.
  32. Papanikolaou P, Swanson G, Stathakis S, Mavroidis P. NTCP modeling and dose-volume correlations of significant hematocrit drops 3 months after prostate radiation therapy. *Adv Radiat Oncol.* 2024;9:101393.
  33. Elumalai T, Periasamy K, Rajendran I, et al. A systematic review of radiation-related lymphopenia in genito-urinary malignancies. *Cancer Invest.* 2021;39:769-776.
  34. Iorio GC, Spieler BO, Ricardi U, Dal Pra A. The impact of pelvic nodal radiotherapy on hematologic toxicity: a systematic review with focus on leukopenia, lymphopenia and future perspectives in prostate cancer treatment. *Crit Rev Oncol Hematol.* 2021;168:103497.
  35. Pavarini M, Alborghetti L, Aimonetto S, et al. Pelvic bone marrow dose-volume predictors of late lymphopenia following pelvic lymph node radiation therapy for prostate cancer. *Radiother Oncol.* 2024;195:110230.
  36. Schad MD, Dutta SW, Muller DM, Wijesooriya K, Showalter TN. Radiation-related lymphopenia after pelvic nodal irradiation for prostate cancer. *Adv Radiat Oncol.* 2019;4:323-330.
  37. Bresolin A, Garibaldi E, Faiella A, et al. Predictors of 2-year incidence of patient-reported urinary incontinence after post-prostatectomy radiotherapy: evidence of dose and fractionation effects. *Front Oncol.* 2020;10:1207.
  38. Bresolin A, Faiella A, Garibaldi E, et al. Acute patient-reported intestinal toxicity in whole pelvis IMRT for prostate cancer: bowel dose-volume effect quantification in a multicentric cohort study. *Radiother Oncol.* 2021;158:74-82.
  39. Roach M, Marquez C, Yuo HS, et al. Predicting the risk of lymph node involvement using the pre-treatment prostate specific antigen and Gleason score in men with clinically localized prostate cancer. *Int J Radiat Oncol Biol Phys.* 1994;28:33-37.
  40. Wasserthal J, Breit HC, Meyer MT, et al. TotalSegmentator: robust segmentation of 104 anatomic structures in CT images. *Radiol Artif Intell.* 2023;5:e230034.
  41. Joseph N, McWilliam A, Kennedy J, et al. Post-treatment lymphocytopenia, integral body dose and overall survival in lung cancer patients treated with radical radiotherapy. *Radiother Oncol.* 2019;135:115-119.
  42. Yang L, Xu Z, Ma L, et al. Early onset of severe lymphopenia during definitive radiotherapy correlates with mean body dose and predicts poor survival in cervical cancer. *Cancer Biomark.* 2022;34:149-159.
  43. Joseph N, Cicchetti A, McWilliam A, et al. High weekly integral dose and larger fraction size increase risk of fatigue and worsening of functional outcomes following radiotherapy for localized prostate cancer. *Front Oncol.* 2022;12:937934.
  44. National Cancer Institute. *National Institutes of Health, US Department of Health and Human Services. Common Terminology Criteria for Adverse Events (CTCAE) Version 4.0* Published May 28, 2009. Revised version 4.03 June 14, 2010.
  45. Collins GS, Reitsma JB, Altman DG, et al. Transparent reporting of a multivariable prediction model for individual prognosis or diagnosis (TRIPOD): the TRIPOD statement. *BMC Med.* 2015;350:g7594.
  46. Steyerberg EW. *Clinical Prediction Models*. 2nd ed. Nature Switzerland AG: Springer; 2019.
  47. Austin PC, Steyerberg EW. Events per variable (EPV) and the relative performance of different strategies for estimating the out-of-sample validity of logistic regression models. *Stat Methods Med Res.* 2017;26(2):796-808.
  48. Pinkawa M, Djukic V, Klotz J, et al. Hematologic changes during prostate cancer radiation therapy are dependent on the treatment volume. *Future Oncol.* 2014;10:835-843.
  49. Miszczyk M, Majewski W. Hematologic toxicity of conformal radiotherapy and intensity modulated radiotherapy in prostate and bladder cancer patients. *Asian Pac J Cancer Prev.* 2018;19:2803-2806.
  50. De Ornelas M, Iorio GC, Bossart E, et al. Bone marrow sparing in prostate cancer patients treated with Post-operative pelvic nodal radiotherapy - a proton versus photon comparison. *Phys Med.* 2023;112:102644.
  51. Baré M, Poeta S, Fernandes P, et al. Lymphocyte-sparing pelvic radiotherapy for prostate cancer: an in-silico study. *Phys Imaging Radiat Oncol.* 2022;23:127-133.
  52. Whitaker TJ, Routman DM, Schultz H, et al. IMPT versus VMAT for pelvic nodal irradiation in prostate cancer: a dosimetric comparison. *Int J Part Ther.* 2019;5(3):11-23.
  53. Widesott L, Pierelli A, Fiorino C, et al. Intensity-modulated proton therapy versus helical tomotherapy in nasopharynx cancer: planning comparison and NTCP evaluation. *Int J Radiat Oncol Biol Phys.* 2008;72(2):589-596.
  54. Ebert MA, Gulliford S, Acosta O, et al. Spatial descriptions of radiotherapy dose: normal tissue complication models and statistical associations. *Phys Med Biol.* 2021;66(12). <https://doi.org/10.1088/1361-6560/ac0681>.